

OBSERVED BEHAVIOR OF RECTANGULAR RC COLUMNS CONFINED WITH CFRP JACKETS AND ANCHORS

José Luis JIMÉNEZ¹, Hernán SANTA MARÍA²

ABSTRACT

Twelve rectangular reinforced concrete columns were constructed to study the behavior of a proposed confinement system. The confinement system is composed of CFRP wraps and CFRP anchors installed with an intercalated disposition. Eight of these columns are reinforced with the proposed system, while four are left without CFRP confinement to evaluate the increments on the axial stress-strain properties due to the CFRP confinement. The specimens were instrumented to capture average axial deformations, total applied load, CFRP deformations with strain gages and with a digital image correlation (DIC) technique.

Keywords: CFRP confinement; CFRP jackets; CFRP anchors; wall-like columns; reinforced concrete

1. INTRODUCTION

Ductility is perhaps the most influential property of structures located in regions with high seismic activity. Moderate to great earthquakes impose on buildings deformations that could easily exceed elastic behavior. Therefore, resisting systems must be designed to respond in the inelastic domain while sustaining a high portion of their initial strength to minimize severe damage and avoid collapse (Paulay & Priestley, 1992).

FRP – confinement retrofit is a powerful technique to achieve the desired ductility in damaged structural walls or walls susceptible to brittle behavior. The main motivation of the current research is to explore the application of CFRP – confinement to structural walls by studying the behavior of rectangular reinforced concrete columns confined with CFRP jackets and anchors.

FRP can provide a passive type of confinement to concrete. That means that as concrete is subject to axial compression it expands laterally producing a passive confining pressure from the FRP jacket system. Although it is generally accepted that confined concrete has significantly more strength and ductility than unconfined concrete, the relationship between the axial strain and axial stress of FRP – confined concrete is not fully understood due to the many parameters involved.

The present study arises from a previous investigation that tested CFRP anchor confinement without CFRP jackets (Alcaino et al., 2015). Recently, the combination of FRP jackets and anchors has showed to be a powerful technique to increase strength and ductility of rectangular columns. However, very few researchers have studied the behavior of rectangular columns with simultaneous FRP jackets and anchors. One investigation proposes a model for the complete stress – strain curve (Hany, Hantouche, & Harajli, 2016), one proposes a model to predict the compressive strength of confined concrete (Triantafyllou et al., 2016) and three other papers provide with an experimental test data set of

¹MSc Student, Department of Structural and Geotechnical Engineering, Pontificia Universidad Católica de Chile, Santiago, Chile, jjimene@uc.cl

²Associate Professor, Department of Structural and Geotechnical Engineering, Pontificia Universidad Católica de Chile and National Research Center for Integrated Natural Disaster Management CONICYT/FONDAP/15110017, Santiago, Chile, hsm@ing.puc.cl

5 columns (Akgun, Demir, & Ilki, 2010), 5 columns (Ilki et al., 2008) and 3 columns (Tan, 2002) confined with FRP jackets and anchors.

The present investigation experimentally studies the behavior of twelve rectangular reinforced concrete columns (eight with CFRP-confinement and four without CFRP-confinement). The main objectives of the investigation are to study the increases in the stress-strain curve parameters due to the proposed CFRP-confinement and the stresses generated on the CFRP system.

2. EXPERIMENTAL PROGRAM

2.1 Description of Specimens

A total of twelve rectangular reinforced concrete columns were tested to pure axial monotonic compression to failure. The twelve specimens consisted of four control specimens with no CFRP reinforcement and eight specimens strengthened with CFRP jackets and CFRP anchors.

All specimens present a prismatic shape, with 60 cm in height and 40 cm in width. Half of the specimens had a thickness of 15 cm and half a thickness of 10 cm. While the corners of the CFRP-strengthened columns were manually rounded to a minimum 2 cm radius, the corners of the control columns were not rounded. CFRP wraps were placed 5 cm from the top and the bottom of the column). Precast holes were located inside the columns for the installation of the CFRP anchors; these holes had a diameter of 1.6 cm and round edges with a minimum 1 cm radius.

The same materials were used for CFRP jackets and for CFRP anchors. The CFRP jacket and anchors were installed in an intercalated manner beginning and ending with a jacket layer, meaning that an anchor layer was always located between two jacket layers (Figure 1).

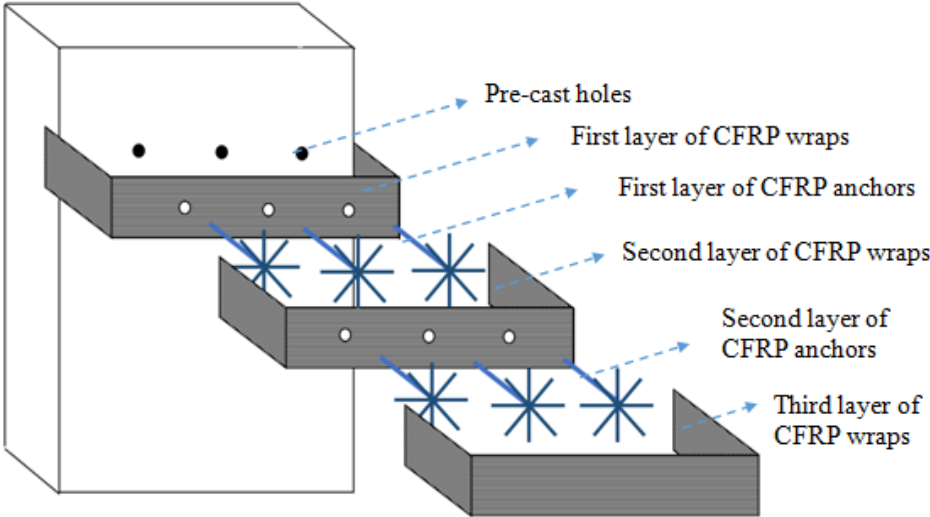


Figure 1. Layout of CFRP reinforcement. CFRP anchors are intercalated between CFRP

Specimens were named according to the nomenclature “ncr-XX”. Figure 2 shows specimen (335-10) to illustrate the nomenclature. In this example “n” equals 3, which indicates that the specimen has 3 layers of CFRP jackets. Since CFRP anchors are installed between CFRP jackets, then the number of CFRP anchor layers is n-1 (for this example that number is 2). The letters “c” and “r” represent the number vertical and horizontal lines of CFRP anchors (3 and 5 in this example). Finally, the letters “XX” indicate the thickness of the column in cm.

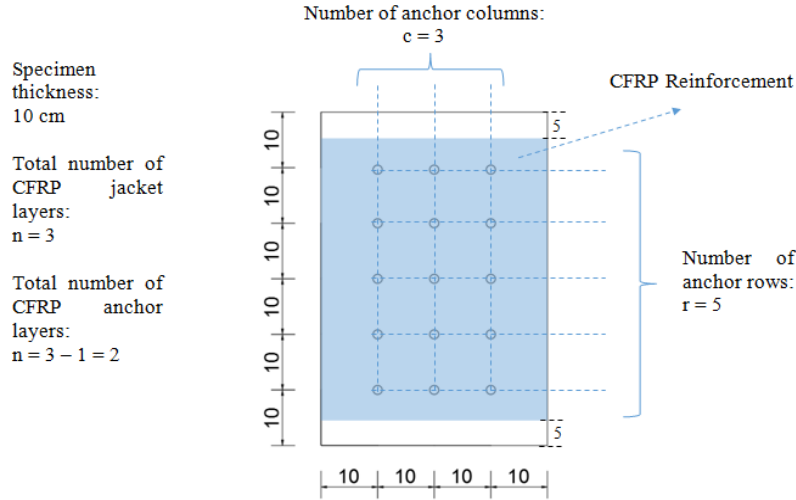


Figure 2. Example of alphanumeric code for column 335-10

2.2 Materials

The specimens were composed of three materials: concrete, steel and the CFRP reinforcement.

The same concrete was used for all specimens. The tested unconfined strength at 28 days of age f_{c-28} was 23.1 MPa. Due to delays in the availability of the testing machine and CFRP materials, the specimens were tested in average at 465 days of age. Therefore, the unconfined strength of concrete at the time of testing was no longer f_{c-28} but a higher value. The unconfined strength and the modulus of elasticity were measured to be 37 MPa and 22180 MPa, respectively, at the day of testing. These parameters were measured by extracting and testing cylinder probes from remaining not-tested specimens.

The same type of steel was used for all specimens with the following nominal mechanical properties: minimum tensile yield stress of 420 MPa, maximum tensile yield stress 580 MPa and minimum tensile ultimate stress of 630 MPa.

Carbon fiber reinforced polymer (CFRP) reinforcement was provided by Simpson Strong-Tie. The same type of CFRP was used for all CFRP strengthened specimens. Properties of the cured composite material are presented in Table 1 according to the manufacturer specifications.

Table 1. Cured composite properties (CSS-UCF10).

Tensile strength	Tensile modulus	Rupture elongation	Thickness per layer
970 MPa	76 GPa	1.3%	0.5 mm

2.3 Specimens Properties

A summary of the parameters of each specimen is presented in Table 1. This Table details the number of vertical bars, the volumetric ratio of vertical bars (ρ_s^v), the transverse bar disposition, the volumetric ratio of transverse bars (ρ_s^h), the ratio of effectively confined area due to steel confinement (κ_s^{shape}), the volumetric ratio of CFRP confinement (ρ_{cfpr}) and the ratio of effectively confined area due to steel confinement ($\kappa_{\text{cfpr}}^{\text{shape}}$).

For all specimens, κ_s^{shape} and $\kappa_{\text{cfpr}}^{\text{shape}}$ are calculated assuming the typical arching action for confinement (Mander et al., 1988). Table 2 shows that the effectively confined area due to CFRP confinement tends

to be significantly larger than the effectively confined area due to transverse bars.

The specimens were tested under uniaxial monotone compression until failure with the use of a forced controlled testing machine. The specimens were instrumented with vertical and horizontal LVDTs in addition to strain gages (Figure 3) and a Digital Image Correlation system.

Table 2. Summary of specimen parameters

Specimen	Ver. Bars (mm)	ρ_s^l	Trans. Bars (mm)	ρ_s^h	κ_s^{shape}	ρ_{cfRP}	κ_{cfRP}^{shape}
000-10a	8 ϕ 10	0.01571	ϕ 6 @ 100	0.0014	0.0138	0	0
000-10b	8 ϕ 10	0.01571	ϕ 6 @ 100	0.0014	0.0138	0	0
000-15a	8 ϕ 12	0.01508	ϕ 6 @ 100	0.0010	0.0491	0	0
000-15b	8 ϕ 12	0.01508	ϕ 6 @ 100	0.0010	0.0491	0	0
225-10	8 ϕ 10	0.01584	ϕ 6 @ 100	0.0014	0.0139	0.0277	0.3033
225-15	8 ϕ 12	0.01517	ϕ 6 @ 100	0.0010	0.0494	0.0210	0.4894
235-10	8 ϕ 10	0.01584	ϕ 6 @ 100	0.0014	0.0139	0.0290	0.3891
235-15	8 ϕ 12	0.01517	ϕ 6 @ 100	0.0010	0.0494	0.0222	0.6414
325-10	8 ϕ 10	0.01584	ϕ 6 @ 100	0.0014	0.0139	0.0429	0.3033
325-15	8 ϕ 12	0.01517	ϕ 6 @ 100	0.0010	0.0494	0.0327	0.4894
335-10	8 ϕ 10	0.01584	ϕ 6 @ 100	0.0014	0.0139	0.0454	0.3891
335-15	8 ϕ 12	0.01517	ϕ 6 @ 100	0.0010	0.0494	0.0352	0.6414

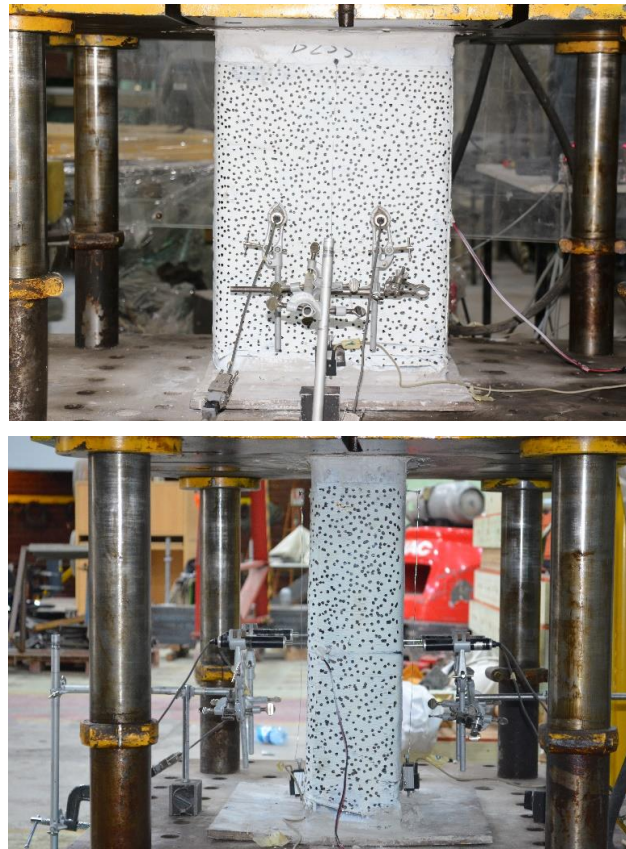


Figure 3. Test setup of specimen 235-15

3. EXPERIMENTAL RESULTS

3.1 Failure Mode

In specimens without CFRP confinement, failure was sudden and explosive, with no indication of cracks prior the explosion. At failure, several concrete fragments were ejected from the specimen at high speeds; LVDTs located at the surface were also ejected at high speeds. Most columns without CFRP presented a diagonal crack along which buckled vertical bars were observed. Failure occurred just after concrete cover was lost; therefore, transverse steel reinforcement was unsuccessful in providing confinement and ductility to the columns. Vertical bars buckled with an effective length larger than the separation between stirrups. As an example, the failure mode of specimen 000-15a is shown in Figure 4a.

In specimens with CFRP confinement, failure was not explosive and was characterized by a progressive and localized rupture of the CFRP reinforcement. The failure zone usually started at one corner, and then propagated vertically and horizontally through the complete width of the column. No other fractures of the CFRP were observed outside of the failure zone. After failure, crushed concrete came out of the failure zone; however, concrete fragments were not ejected at high speed. Concrete outside the failure zone remained uncracked. Since the specimen was fully wrapped with CFRP confinement, no loss of concrete cover was experienced. Vertical steel bars located at the failure zone buckled, while CFRP confinement prevented vertical bar buckling outside the failure zone. Buckled bars at the failure zone presented an effective length close to the height of the CFRP rupture. CFRP anchors located at the fracture zone were usually broken near the edges of the precast holes. As an example, the failure mode of specimen 335-10 is shown in Figure 4b.

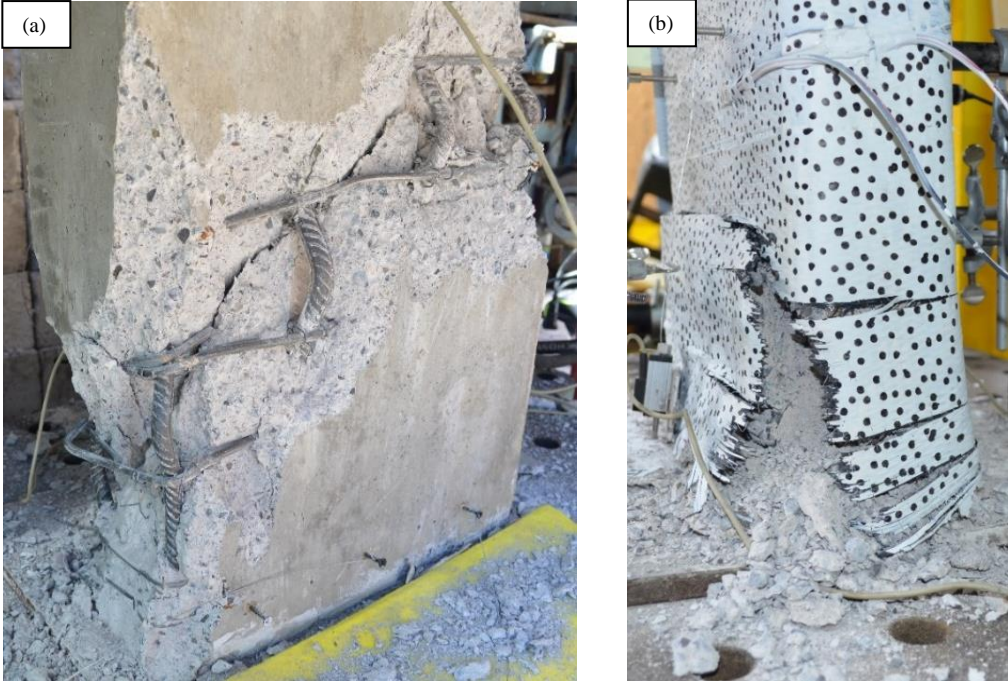


Figure 4. (a) Failure mode of specimen 000-15a and (b) failure mode of specimen 335-10

3.2 Axial Behavior

Figures 5, 6, 7 and 8 show the axial compression stress of concrete vs the average axial strain experimentally obtained for all specimens. To calculate the stress of the concrete an elastic-perfectly plastic behavior is assumed for the longitudinal bars since the axial strain is small enough to neglect hardening.

It is important to mention that since a force-controlled testing machine is used, an uncontrolled rate of displacement is applied. It is possible that the testing machine produced failure of the specimen too fast to be captured with the testing equipment. For this reason, the last portion of the curves present conservative values of the actual deformation capacity of the confined columns.

The curves obtained from specimens with and without CFRP present similar shape, but curves of CFRP confined specimens present a greater strength and ultimate deformation. In general, a larger value of maximum stress was obtained with the 3x5 CFRP anchor disposition than with the 2x5, except for columns 225-10 and 235-10 where specimen 225-10 presented a larger maximum stress. These columns may have been the exception due to the small cross-section area in addition to the few CFRP layers. The ultimate strain did not depend on the CFRP anchor disposition, columns 235-15 and 235-10 achieved a higher ultimate strain than their counterparts 225-15 and 225-10, but columns 335-15 and 335-10 achieved a similar ultimate strain than their counterparts 325-15 and 325-10.

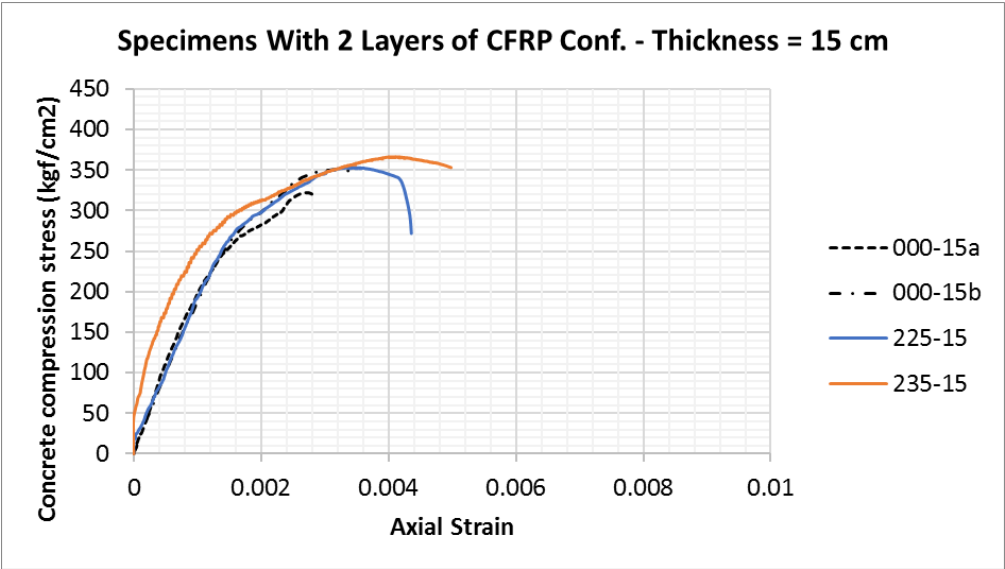


Figure 5. Experimental axial concrete stress vs average axial strain for specimens with 2 layers of CFRP wrapping (15 cm in thickness)

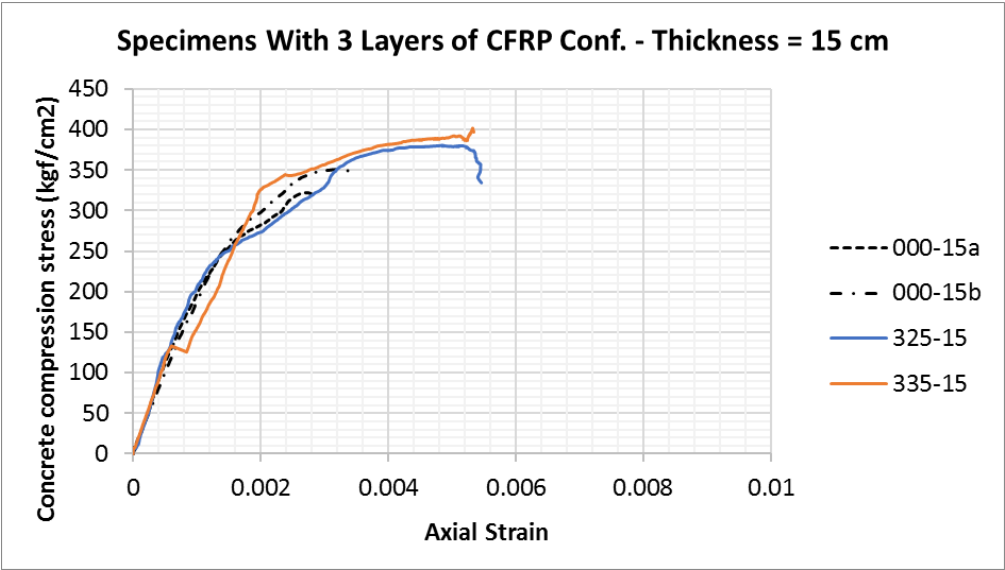


Figure 6. Experimental axial concrete stress vs average axial strain for specimens with 3 layers of CFRP wrapping (15 cm in thickness)

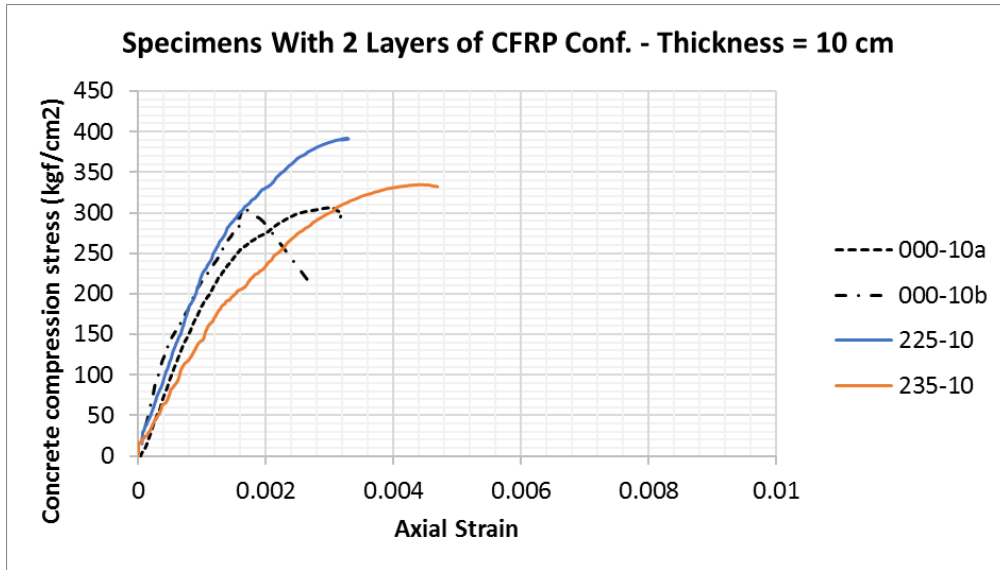


Figure 7. Experimental axial concrete stress vs average axial strain for specimens with 2 layers of CFRP wrapping (10 cm in thickness)

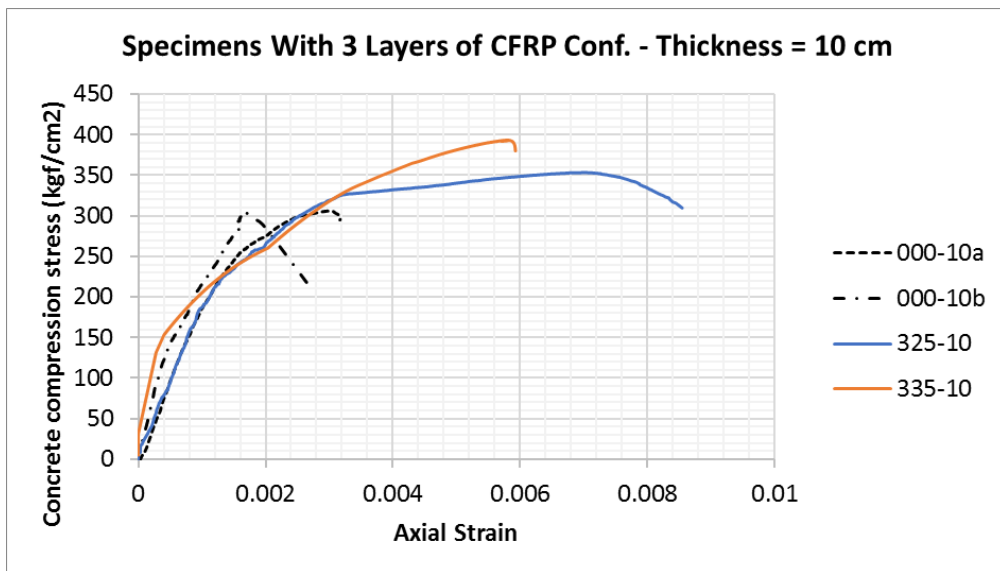


Figure 8. Experimental axial concrete stress vs average axial strain for specimens with 3 layers of CFRP wrapping (10 cm in thickness)

A summary of the parameters obtained from Figures 5 to 8 is presented in Table 3. In this Table, P_{max} stands for the maximum load applied during the tests, f_c^{max} stands for the maximum estimated concrete stress, ϵ_c^{max} stands for the average measured axial strain corresponding to f_c^{max} , E_c stands for the average secant modulus of elasticity, P_{ult} stands for the last load just before the end of the test, f_c^{ult} stands for the estimated concrete stress just before the end of the test (considering an elastic perfectly plastic constitutive for the longitudinal bars), ϵ_c^{ult} stands for the average axial strain corresponding to f_c^{ult} and finally ϵ_{cfpr}^{max-sg} and ϵ_{cfpr}^{ult-sg} stand for the horizontal CFRP strains (captured by strain gages located at the corner (C) and/or middle (M) side of the column on the external CFRP wraps) corresponding to f_c^{max} and f_c^{ult} , respectively. Specimen 335-15 did not reach failure because its strength was higher than the maximum capacity of the testing machine, therefore, parameters P_{ult} , f_c^{ult} , ϵ_c^{ult} and E_D could not be obtained for this specimen.

Table 3. Summary of specimen results related to the axial stress-strain curve

Specimen	P_{max}	f_c^{max}	ϵ_c^{max}	E_c	P_{ult}	f_c^{ult}	ϵ_c^{ult}	ϵ_{CFRP}^{max-sg}	ϵ_{CFRP}^{ult-sg}
	tonf	kgf/cm ²		kgf/cm ²	tonf	kgf/cm ²			
000-10a	147	306	0.0030	190044	143	295	0.0032	-	-
000-10b	142	304	0.0017	269342	110	212	0.0027	-	-
225-10	180	392	0.0032	222739	179	390	0.0033	C: 0.0004	C: 0.0004
235-10	157	334	0.0044	142665	157	332	0.0047	C: 0.0005	C: 0.0005
325-10	165	353	0.0070	191975	148	310	0.0085	C: 0.0051 M: 0.0064	C: 0.0054 M: 0.0055
335-10	180	393	0.0058	221280	175	380	0.0059	C: 0.0000 M: 0.0009	C: 0.0000 M: 0.0008
000-15a	229	322	0.0027	210358	227	319	0.0028	-	-
000-15b	246	351	0.0032	188153	243	346	0.0035	-	-
225-15	246	353	0.0034	193278	198	272	0.0044	C: 0.0006	C: 0.0010
235-15	254	366	0.0041	340588	246	353	0.0050	C: 0.0014	C: 0.0011
325-15	262	380	0.0048	217056	235	334	0.0055	C: 0.0022 M: 0.0007	C: 0.0040 M: 0.0015
335-15	275	401	0.0053	153208	-	-	-	C: 0.0008 M: 0.0025	C: 0.0008 M: 0.0025

Finally, Table 4 presents a summary of the ratios of the measured stress-strain parameters of the CFRP confined columns divided by the respective average of the measured values of the specimens without CFRP confinement.

Table 4. Summary of ratios of parameters due to CFRP confinement

Specimen	Δf_c^{max}	$\Delta \epsilon_c^{max}$	ΔE_c	Δf_c^{ult}	$\Delta \epsilon_c^{ult}$
225-10	1.29	1.33	0.97	1.54	1.10
235-10	1.10	1.83	0.62	1.31	1.57
325-10	1.16	2.92	0.84	1.22	2.83
335-10	1.29	2.42	0.96	1.50	1.97
225-15	1.05	1.13	0.97	0.82	1.38
235-15	1.09	1.37	1.71	1.06	1.56
325-15	1.13	1.60	1.09	1.00	1.72
335-15	1.19	1.77	0.77	-	-
Average	1.16	1.80	0.99	1.21	1.73
Stan. Dev.	0.09	0.60	0.32	0.27	0.55

From these results, it is observed that a larger increase in concrete maximum stress and ultimate strain was obtained when a larger number of CFRP wraps and anchors was used. The initial secant concrete stiffness of CFRP confined columns is on average 88% of the control specimens (ignoring specimen 235-15, since its vertical LVDTs could not capture the initial portion of the curve). This is mainly due to the presence of pre-cast holes that were not refilled after CFRP installation. Pre-cast holes were not refilled because introduction of epoxy into the cavities was blocked by the CFRP wraps. A more efficient CFRP installation technique needs to be developed to allow pre-cast holes refill.

3.3 CFRP Stresses

3.3.1 Strain Gages

A total of 12 strain gages were distributed among the columns with CFRP reinforcement. Two strain gages were placed on each of the specimens with three layers of CFRP wraps (325-15, 325-10, 335-15 and 335-10), one at the corner at mid height and one 12 cm from the edge at the same height. One strain gage was placed on each of the specimens with two layers of CFRP wraps (225-15, 225-10, 235-15 and 235-10) located at the corner of the specimen at mid height.

Figure 9 shows the measured CFRP strains through the test for a strain gage located at a corner inside the failure zone (Figure 9a) and for a strain gage located at a corner outside the failure zone (Figure 9b).

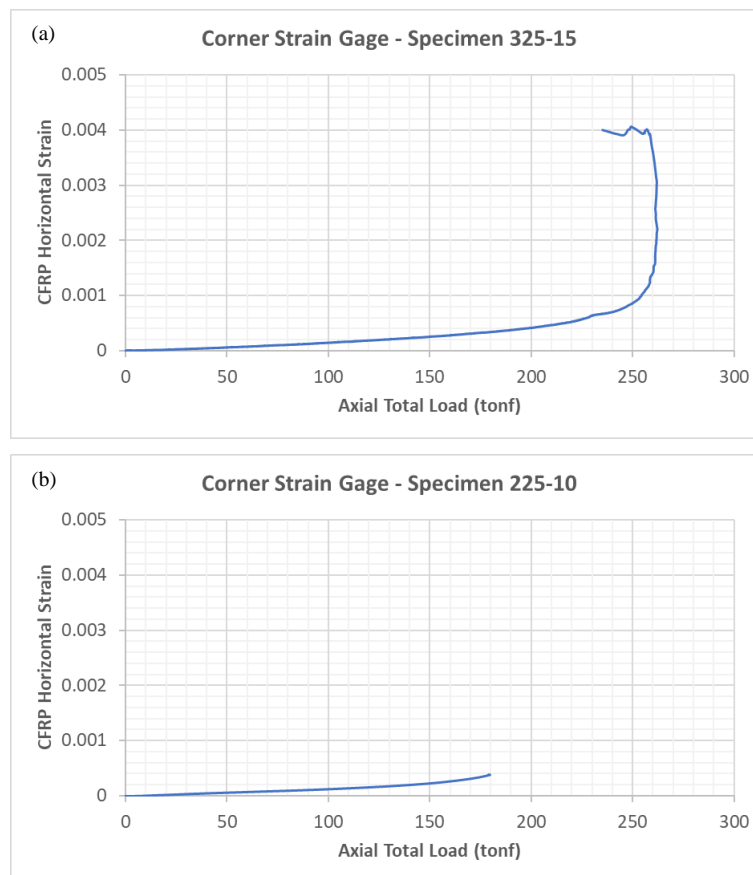


Figure 9. CFRP strain vs axial load, strain gage located at a corner: (a) inside failure zone (Specimen 325-15), (b) outside failure zone (Specimen 225-10)

Strain gage readings showed that CFRP strain distribution is highly heterogeneous, presenting localized zones with strains high enough to generate CFRP rupture and other zones with considerably smaller strains. Also, most of the CFRP confinement system presents very small strain until the maximum concrete stresses is reached, after this point strain in the CFRP wraps increase exponentially.

3.3.2 Digital Image Correlation (DIC)

To capture the complete field of deformations a technique of image data correlation is used. For this purpose, two adjacent sides of the specimens were painted white and numerous random black dots were marked over the two sides of the specimens. With the use of two digital cameras, photographs

were taken of these two sides every 5 seconds while the test took place. The photographs were used to determine the deformation field of the outer CFRP layer with the use of Optical Digital Image Correlation software (Barthes, n.d.).

As an example, the strains calculated with this technique for specimen 335-15 are presented in Figure 10. These graphics show the field of strains in the horizontal direction (Figure 10a) and vertical direction (Figure 10b) at the closest instant before failure of the specimen. All the strains showed in these figures were calculated for the last step prior to failure of the column.

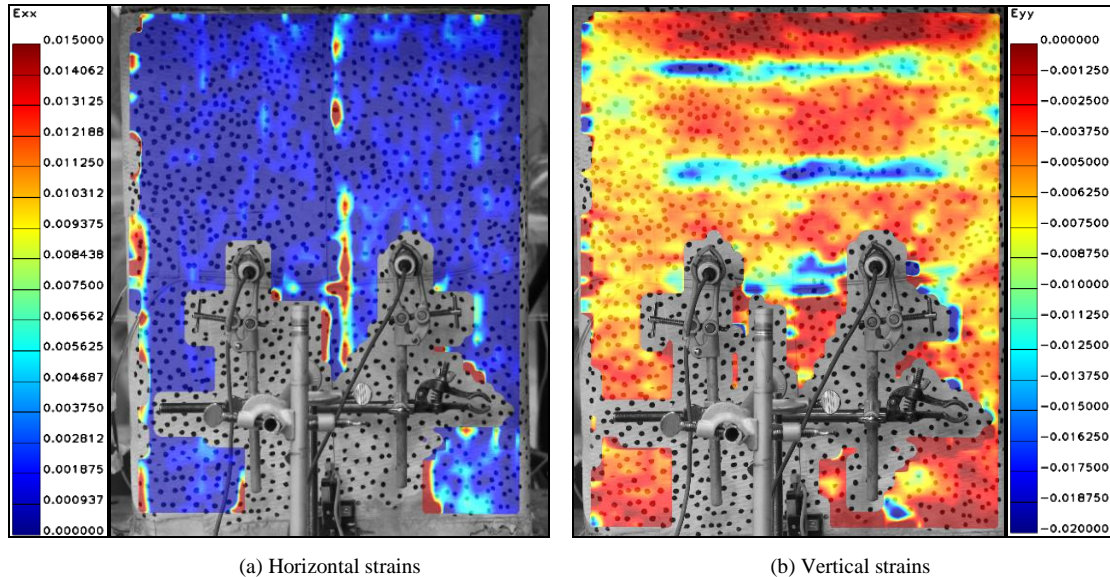


Figure 10. Strains immediately before failure, captured by DIC for specimen 335-15

Digital image correlation was able to detect high strains in at the failure zone; however, the strains detected tend to be overestimated. Values as higher than 0.01 were calculated using DIC, which cannot be possible since the manufacturer specified 0.013 as the ultimate CFRP strain on a tension test. Ultimate strain of installed CFRP should be a fraction of ultimate strain in pure tension. DIC overestimation might be explained by the rate the photographs were taken (1 photographs every 5 seconds) and re-accommodation of CFRP wraps. Higher speed photographs are required to obtain strain fields closer to the rupture instant. It is also possible that some air bubbles were trapped between CFRP layers, and therefore a portion of the displacements captured with the photographs could have been the translations of the fibers after the expulsion of the air and not strain related to a stress state.

4. CONCLUSIONS

Following are the principal conclusions obtained from the construction and testing of these columns:

- The alternated disposition of CFRP anchors and CFRP wraps generated a strong joint between all CFRP components. None of the columns failed by deboning of the CFRP components. All columns presented initially rupture of the CFRP at the corners of the column and then progressed to anchors near the edges of the pre-cast holes.
- The columns confined with CFRP experienced larger maximum stress, ultimate stress and ultimate strain than their corresponding control columns. CFRP confined columns maintained the maximum stress while experiencing axial deformation, generating energy dissipation and ductility.
- After the first CFRP fiber ruptured, the load of the column dropped abruptly but the integrity of the columns remained throughout the complete loading. Buckling of vertical bars was observed only at

failure zones and opening of stirrups was not observed in CFRP confined specimens.

- The complex geometry of the CFRP reinforcement produced the introduction of air bubbles inside the CFRP system. Although the presence of bubbles reduced the efficiency of the confining system, the CFRP confining stresses were sufficient to generate an increase in ductility.
- Independent if strain gages were located inside or outside the failure zone, deformation in the CFRP confinement was observed to be small before the maximum load was reached and increased rapidly after the maximum load was reached.
- Although digital image correlation tends to overestimate the field of deformations on the outer layer of CFRP, this technique is successful in identifying the location of the failure zone.
- Since a force controlled testing machine was used, only a small portion of the descending branch was captured, and increments in f_c^{ult} and ϵ_c^{ult} could have been larger if a displacement testing machine was used.

5. ACKNOWLEDGMENTS

The authors wish to thank Matias Urrejola from Simpson Strong Tie for providing the CFRP material used for this investigation and the Laboratory of Structural Engineering at the Pontificia Universidad Católica de Chile for providing the means for completing the present investigation.

6. REFERENCES

- Akgun D, Demir C, & Ilki A (2010). Axial behavior of FRP jacketed extended rectangular members constructed with low strength concrete. *Proceedings of the 5th International Conference On FRP Composites In Civil Engineering*, Beijing, China.
- Alcaino P, Santa María H, Cinquia A, Invernizzi S (2015). Confinement of reinforced concrete compression members using bowtie CFRP reinforcement. *Proceedings of the XI Chilean Congress of seismology and earthquake engineering*. Santiago, Chile.
- Barthes C (n.d.). Optecal digital image correlation software. Retrieved December 29, 2017, from <http://optecal.com/>
- Hany N F, Hantouche E G, Harajli M H (2015). Axial stress-strain model of CFRP-confined concrete under monotonic and cyclic loading. *Journal of Composite Construction*, 19(6).
- Hany N F, Hantouche E G, Harajli M H (2016). Generalized axial stress-strain response of rectangular columns confined using CFRP jackets and anchors. *Journal of Composite Construction*, 21(1).
- Ilki A, Peker O, Karamuk E, Demir C, Kumbasar N (2008). FRP retrofit of low and medium strength circular and rectangular reinforced concrete columns. *Journal of Materials in Civil Engineering*, 20(2): 169 - 188.
- Mander J B, Priestley M, Park R (1988a). Theoretical stress - strain model for confined concrete. *Journal of Structural Engineering*, 114(8): 1804 - 1826.
- Paulay T, Priestley M (1992). *Seismic design of reinforced concrete and masonry buildings*, John Wiley & Sons, Inc, New York.
- Tan K H (2002). Strength enhancement of rectangular reinforced concrete columns using fiber-reinforced polymer. *Journal of Composite Construction*, 6(3): 175 - 183.
- Triantafyllou T C, Choutopoulou E, Fotaki E, Skorda M, Stathopoulou M, Karlos K (2016). FRP confinement of wall-like reinforced concrete columns. *Materials and Structures*, 49(1): 651 - 664.